RGNZ/MGPB

Mathematical Determination of Rock Joints Morphological Profile

Rudarsko-geološko-naftni zbornik
(The Mining-Geology-Petroleum Engineering Bulletin)
UDC: 622.2
DOI: 10.17794/rgn.2022.2.10

Original scientific paper

Jamal Zadhesh[1], Abbas Majdi[2]

[1] *School of Mining, College of Engineering, University of Tehran, Tehran, Iran, j.zadhesh@ut.ac.ir, ORCID iD: 0000-0002-9115-3998*
[2] *School of Mining, College of Engineering, University of Tehran, Tehran, Iran, amajdi@ut.ac.ir, ORCID iD: 0000-0002-4167-7814*

Abstract

Determining the geometric or morphology and mechanical properties of joints and geomechanics of intact rock is a vitally important issue in predicting the behaviour of structures built inside or on rock masses. The joint morphology is significant because it affects the strength of the rock mass and controls the stability of the structures related to the rock masses. Until recently, joint morphology was introduced in a simple form which brought about models that are far from the inherent state of a rock joint. The work presented in this research introduces a new model to represent rock joint morphology which is very close to reality. For this research, Sarchawa marble mine joint systems are studied. According to this research, the morphology of each rock joint can be expressed as a mathematical equation. Using the output of this research, we can see a more realistic view of the rock masses. As a result, we can have better designs for structures correlated to rock masses, making the result better and more reliable.

Keywords:
rock masses; joint morphology; mathematical equation; Sarchawa marble mine.

1. Introduction

Flaws make the world beautiful; without the drawbacks, rocks and mountains would have been perfectly boring (**Griffith, 1921**). Knowing the type and quantity of rock defects is more important than knowing the rock itself (**Terzaghi, 1946**). The purpose of any research is to better understand the world around us. When we know the world around us, we will be more successful in solving possible problems in the world. In rock engineering, we deal with rock masses, so we must have a realistic view of the rock masses.

Rock discontinuities control rock mass structures by changing the mechanical properties of rock masses. The mechanical properties of jointed rock masses depend on the rock's mechanical properties and the joints' geometrical characteristics (**Grasselli and Egger, 2003; Park and Song, 2009**). Rock joint networks and their geometrical properties are the most significant factors in rock masses' permeability, deformability, strength, and stability (**Hudson and Harrison, 1997**). The most critical issue in rock mechanics to model rock masses is to obtain the three-dimensional state of the rock mass using the received data (**Flynn and Pine, 2007**), so the success of this issue is due to a geometrical model of the rock joints.

Most of the world is made of rock, and most rock near the surface is fractured. The fractures dominate the rock mass geometry, deformation modulus, strength, failure behaviour, permeability, and even the local magnitudes and directions of the in-situ stress field. Understanding the presence and mechanics of the discontinuities, both singly and in the rock mass context, is therefore of paramount importance to civil, mining, and petroleum engineers (**Priest, 1993**). So, on-site characterization of a rock exposure for a project is essential in collecting the input data for further rock mechanics analysis, rock engineering design, and numerical modeling. The quality and quantity of the on-site mapping data play an essential role in the results of the following steps. The success of a rock engineering project mainly depends on how well the joints are characterized and considered in the design and construction (**Feng, 2012**). Eventually, in rock engineering, determining the geomechanical properties of jointed rock masses is a critical issue that restricts project design, construction, and operation decisions.

Accurate information about the shape of the joints is deficient because even the extraction of the joints inside the tunnels or even in the rock outcrops does not provide complete information about the shape of the joints. Only precise drilling of a joint does this. In general, the block (prismatic) appearance of rock masses shows polygonal shapes (**Kulander et al., 1979; Barton, 1983**); Circular joints are also created through hydraulic fractures in the laboratory (**Cleary, 1984**).

In most mathematical descriptions, joint shapes within a particular rock mass are considered immutable (**Veneziano, 1978**); however, it introduced a model that

Corresponding author: Jamal Zadhesh
e-mail address: j.zadhesh@ut.ac.ir

Table 1: The Summarizes of the rock joint system models

Model	Joint characteristics considered in the model							
	Shape	Size	Face	Profile	Occurrence	Termination at intersect	Coplanarity	Orientation of sets
Random disk (Santalo, 1976)	Circle, Ellipse	Bounded	Planar	Straight line	Any location	Yes	Yes	Stochastic
Poisson flat (Baecher, 1983	Polygon	Bounded	Planar	Straight line	Any location	Yes	Yes	Stochastic
Orthogonal (Childs, 1957)	Rectangle	Bounded Unbounded	Planar	Straight line	Any location	No Yes	Yes Yes	Parallel Parallel
Baecher (Baecher and Lanney, 1978)	Circle, Ellipse	Bounded	Planar	Straight line	Any location	NO	No	Stochastic
Veneziano (Veneziano, 1978)	Polygon	Bounded	Planar	Straight line	Any location	In joint planes, only	Yes	Stochastic
Dershowitz (Dershwitz, 1984)	Polygon	Bounded	Planar	Straight line	Any location	Yes	Yes	Stochastic
Voronoi (Ambarcumjan, 1974)	Polygon	Bounded	Planar	Straight line	Any location	Yes	Yes	Regular, Stochastic

forms joints through Poisson lines. So, polygon shapes are random. Flat deviation can be described mathematically with appropriate surfaces such as lines, sine, and rotational surfaces. The arbitrary representation of non-flatness on the roughness scale is discussed by (**Roberds, 1979; Swan, 1981**). Yet again, it is difficult to see entirely in three dimensions.

In the field of geoscience engineering, joint models and modeling the jointed rock masses have been a foreground task for some 50 years in various disciplines, especially in mining, and geological science (**Becker et al. 2018; Berkowitz, B., 1995; Wuestefeld et al. 2016; Li et al. 2018; Lavenu and Lamarche 2018**), petroleum, natural gas (**Shakiba et al. 2018**), geothermal, hydrogeology (**Black, 1994; Renshaw, 1998**), geomechanics (**Meyer, Einstein, and Ivanova, 1999**), water resources (**Li et al. 2017b**), nuclear energy, and many other disciplines (**Cacciari and Futai 2017**).

The most important thing to be considered is the actual morphology of the joint because the morphology of the joint affects all calculations of rock engineering designs. The meaning of joint morphology is its proper form. Unfortunately, due to the difficulty of the subject, the actual morphology of the joint has not yet been investigated. Many researchers have presented several simple forms of joint models, which introduced models far from the exact joint morphology.

Until recently, joint morphology was introduced in a simple form such as random-disk, Poisson flat, and Veneziano polygon. None of the presented models have provided a proper mathematical relation for expressing a joint growth equation. All the introduced models simulate the joint profile linearly; this is far from the real inherent state of a rock joint. The drawbacks of the traditional models significantly impact the quantity and quality of joint data and will inevitably affect our understanding of the joint influence on rock mass behaviour.

The work presented in this research introduces a new model to represent rock joint morphology that is very close to reality. This research aims to develop a mathematical model to express joint traces on rock surfaces. The model can show the joint equation, including joint properties, such as length, aperture, roughness, and shape. Consequently, using the obtained information, the two-dimensional structure of the rock mass will be simulated.

2. Review of previous works

A concept or model of the geometry of jointing is needed to develop sampling plans and interpret their results. Ideally, such a model would be specified by a few parameters and simple enough to identify from routine field observations. Several models of fracture geometry have been proposed in various literature. In the following, introduced models will be presented briefly. It must be said that in this study, the profile and plan of the proposed models are considered.

System representations of joints describe the properties of joints as an entity. Since the joints have many geometric properties and a seemingly infinite number of compounds, they can produce a corresponding number of joint system models. Instead, reality shows a relatively limited number of geometric properties of rock masses. The mentioned joint models can accurately represent the geometries of many, though not all, joints. In each model, some features have specific relationships but can be different. (For example, joints orient with an orthogonal exponential distance distribution.) By taking the particle property relationships, joint models can represent rock mass geometry as an entity. **Table 1** summarizes the rock joint system models that are discussed.

Each of these seven models is composed of a specific mixture of features of the rock joint properties. The flatness of the joints is specified as flat for all models, and any joint location and automatic correlation process are allowed in each model. Any component attribute that is selected at random may also be deterministic. For all models, the joints are flat, and any location or autocorrelation process is possible, and the profile of the proposed models is a straight line, which is not possible. The joint's location is usually random. Bounding of joints infers those joints smaller than the area under contemplation can be represented. Joint sizes are typically stochastic, determined directly or indirectly by a random location or orientation. The proposed models cannot identify the morphological characteristics of the joints, so we must introduce a model that is almost an actual model for rock joints.

3. Correlation, Occurrence, and features of joint propagation

According to investigations by researchers, all joint characteristics have been made due to the same mechanism that many of the joint characteristics are autocorrelated (**Matheron, 1975; Agterberg, 1976; Miller, 1979; La Pointe, 1980; Call et al., 1976; Einstein et al., 1980, Zadhesh et al., 2022b, Zadhesh et al., 2022c**). The general trouble in modeling rock masses is that rock is a natural environmental material. So, the physical or engineering properties must be established rather than defined through a manufacturing process (**Harrison and Hudson, 2000**). The complex mixture of ingredients and its long creation history make rock masses an unsuitable material for mathematical depiction via rock mass simulation (**Jing, 2003**).

To understand the behaviour of the joint, it is better to examine how to begin the growth of the joint and its ending. According to the Griffith theory, the beginning and end of the joint propagation and the total opening of the joints are terminated by the spindle shape, and the front and back of the joint are extendable. It can be considered the smallest joint unit by drawing the Griffith joint in an exaggerated form, shown in **Figure 1.**

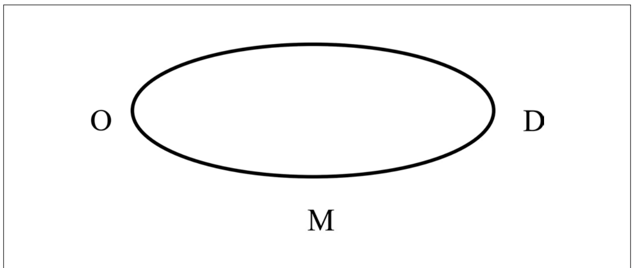

Figure 1: Griffith joint in an exaggerated form

The initial opening of the joint requires high energy consumption. When it reaches its peak, energy consumption will peak, and as a result, in the largest aperture of the joint, a significant drop in energy occurs, and this drop begins from the peak and ends up at the end joint.

When part of the rock is affected by force, it transfers the applied force to other parts; the pressure or stress moves inside the rock. The propagation of stress inside the rock follows the wave propagation rules. The wave propagation in intact rock (i.e. a small sample) is subject to material properties such as the mineral content, the size and shape of the mineral grains, and the presence of pores and microcracks. These properties affect Young's modulus and density of the rock, thus affecting the propagation of P- and S-waves. External factors such as prevailing stresses and degree of saturation also affect the wave propagation in intact rock (**Lama and Vutukuri, 1978**).

A force generates a joint, and depending on the power that creates the joint, the joint wants to grow, but material resistance will prevent the joint growth. Due to the morphology of the joints in various types of rocks, it can be seen that the joints have a wave-like state. Therefore, if we consider the joint as a wave, and according to what has been said, the material's resistance force will prevent the joint's growth, in each period of the development of the joint, both the amplitude and range decrease. So, the resistive force of the material reduces the oscillation of the joint growth equation.

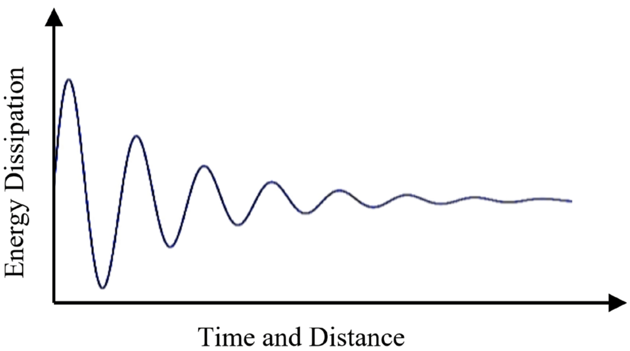

Figure 2: The general form of damping

Figure 3: The wave-like state of joints of the Sarchawa marble mine

Figure 4: A general view of the Sarchawa marble mining quarry (benches and extraction blocks are shown)

Damping will occur. In **Figure 2**, the general form of damping is shown. Also, in **Figure 3**, there are several discontinuities in which a wave-like state can be observed.

To reach a quasi-static equilibrium, it is necessary that the kinetic energy dissipates. Especially when the rock mass study is a highly dynamic approach, damping is required. Finally, it can be said that the discontinuities were formed by forces that had a damping state. Therefore, we need to know the damping forces to better understand discontinuities' behaviour.

4. Description of case study

Sarchawa marble mine is located 18km away from the north of Saqqez in Kurdistan Province in the west of Iran. According to surveys, the mine is situated in the Sanandaj – Sijan regional tectonic zone. As a result, the rock units in this sheet have the Sanandaj – Sijan regional tectonic zone characteristics. The mining quarry has been opened in the marble rock mass. Marble is a metamorphic rock that forms when limestone is subjected to the heat and pressure of metamorphism. It comprises calcite ($CaCO_3$) and usually contains other minerals, such as clay minerals, micas, quartz, pyrite, iron oxides, and graphite. Under the conditions of metamorphism, the calcite in the limestone recrystallizes to form a rock that is a mass of interlocking calcite crystals. A related rock, dolomitic marble, is produced when dolostone is subjected to heat and pressure. Currently, the mining quarry is extracted by one bench divided into several blocks. In **Figure 4**, the bench of the mining quarry is shown (it is worth noting that the bench which is shown in Figure 4 is being studied), and in **Figure 5**, the study area and the geographical location of the open pit in the Sarchawa marble mine are shown.

5. Rock Joint Mapping

Joint surveys are an essential section of site characterization studies in rock engineering because jointed rock masses' strength, deformation, and flow behaviour are strongly influenced by rock joints' geometry and engineering properties (**Liu et al., 2008**).

At this step, all of the joints in the blocks of the extraction bench are mapped by the imaging method, and then, using image processing methods, all the features of the joints are extracted from the taken images. Since the length of the extraction bench is high, the entire block cannot fit into one picture, so several images must be taken to capture all the details of the bench. In **Figure 4**, bench one and extraction blocks are shown. It is worth mentioning that the investigated joints were collected in the Sarchawa marble mine by the corresponding author (Jamal Zadhesh) for his doctoral thesis.

In this section of the study, only the length of joints and their spatial position were studied. First, existing joints and extract information about their situation and length were digitized. Using the digital data of the joints, the Fourier series equations were obtained for all the joints in the extraction blocks of the bench with an acceptable error coefficient. Finally, mathematical equations of joint growth were calculated.

6. Rock Joint Digitizing

All images were processed using image processing techniques. Then all the discontinuities in the photos were digitized, and all their features were extracted. All these tasks were done in MATLAB software. To ensure the correctness of the proposed methodology for conducting research, only the rock joint data of Block 6 was used in this part of the study. The digitized joints in block six are shown in **Figure 6**.

7. Obtaining Fourier series equations of rock joints

A Fourier series is a mathematical method to convert a function into a trigonometric series. The general idea is that a function can be closely described as a summation of sine and cosine waves of different frequencies and amplitudes. The nice thing about the Fourier series is that they still have very close approximations even when

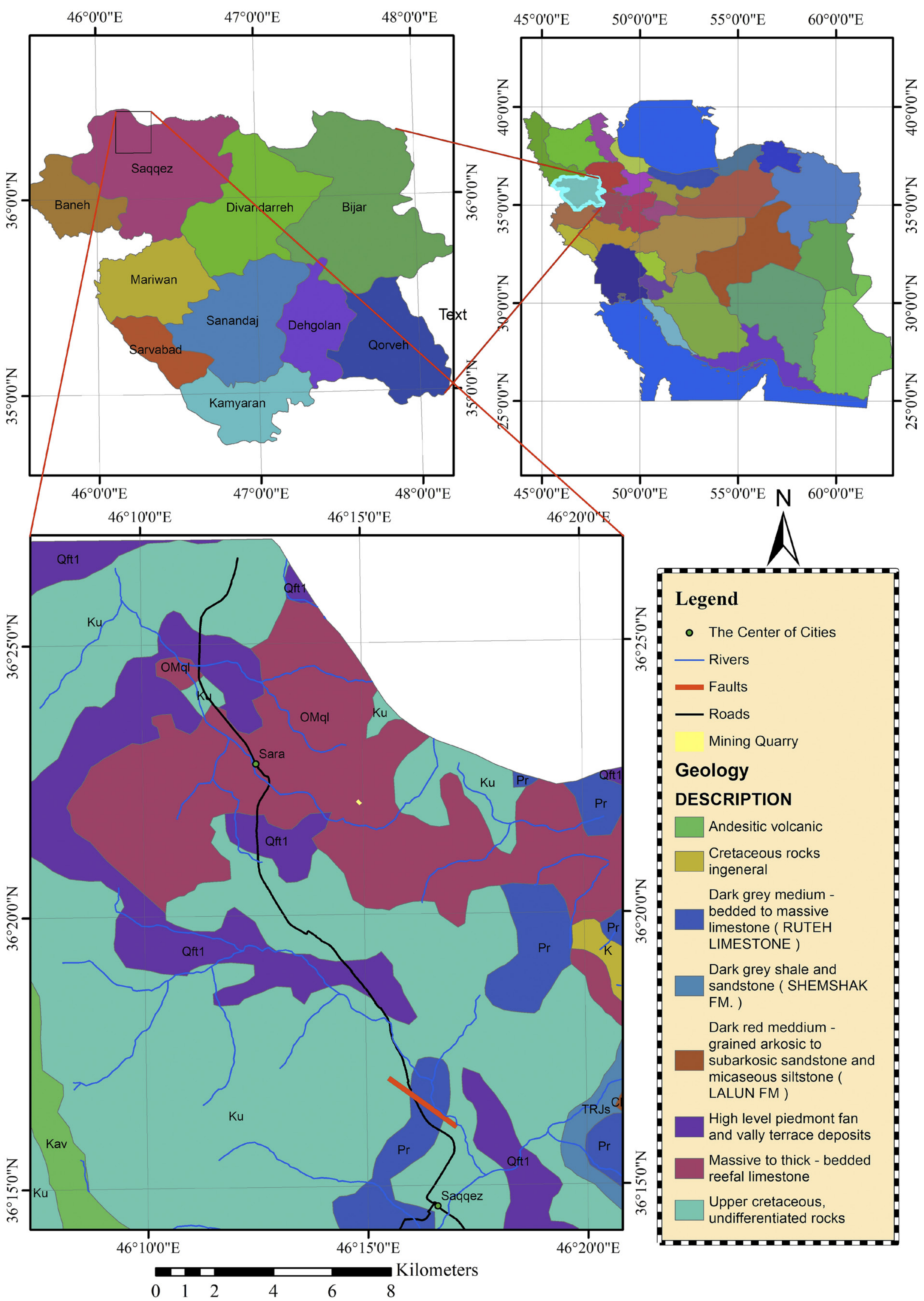

Figure 5: The location of the study area, and the geographical location of the open pit in the Sarchawa marble mine

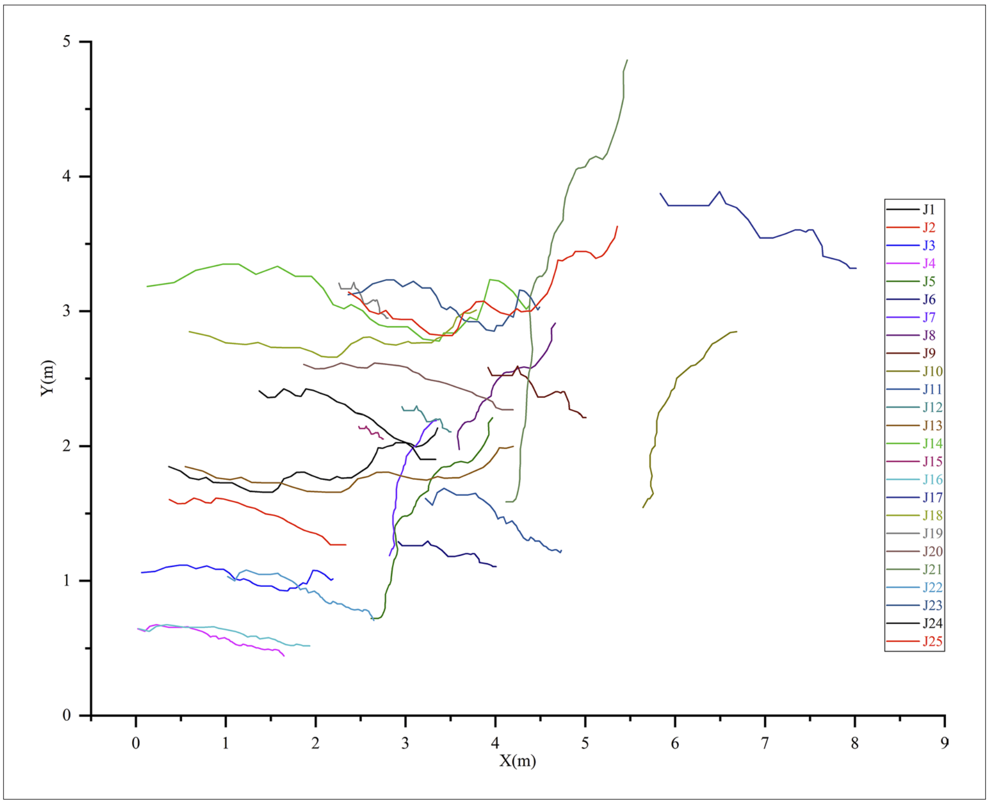

Figure 6: Digitized joints in Block 6 (only those joints are shown, visible on both ends.)

evaluated to a relatively small n^{th} value. A Fourier series is an expansion of a periodic function f(x) in terms of an infinite sum of sines and cosines. A Fourier series uses the orthogonality relationships of the sine and cosine functions. The computation and study of the Fourier series are known as harmonic analysis. They are extremely useful as a way to break up an arbitrary periodic function into a set of simple terms that can be plugged in, solved individually, and then recombined to obtain the solution to the original problem or an approximation to it to whatever accuracy is desired or is practical (**Kreyszig, 1999**).

Using the method for a generalized Fourier series, the usual Fourier series involving sines and cosines is obtained by taking $f_1(x)=\cos(x)$ and $f_2(x)=\sin(x)$. Since these functions form a complete orthogonal system over [-π, π], the Fourier series of a function f(x) is given by **Equation 1**:

$$f(x) = a_0 + \sum_{n=1}^{\infty} a_n \cos(nx) + \sum_{n=1}^{\infty} b_n \sin(nx) \quad (1)$$

Where:

a_0, a_n, b_n – coefficients and calculated according to **Equation 2**:

$$\begin{cases} a_0 = \dfrac{1}{2\pi}\displaystyle\int_{-\pi}^{\pi} f(x)\,dx \\ a_n = \dfrac{1}{\pi}\displaystyle\int_{-\pi}^{\pi} f(x)\cos(nx)\,dx \quad n=1,2,3,\ldots \\ b_n = \dfrac{1}{\pi}\displaystyle\int_{-\pi}^{\pi} f(x)\sin(nx)\,dx \quad n=1,2,3,\ldots \end{cases} \quad (2)$$

For a function f(x) periodic on an interval [-L, L] instead of [-π, π], a simple change of variables can be used to transform the interval of integration from [-π, π] to [-L, L]. By implying **Equation 1**, **Equation 3** is attained, and coefficients can be calculated by **Equation 4**:

$$f(x) = a_0 + \sum_{n=1}^{\infty} a_n \cos\left(\frac{n\pi x}{L}\right) + \sum_{n=1}^{\infty} b_n \sin\left(\frac{n\pi x}{L}\right) \quad (3)$$

$$\begin{cases} a_0 = \dfrac{1}{2L}\displaystyle\int_{-L}^{L} f(x)\,dx \\ a_n = \dfrac{1}{L}\displaystyle\int_{-L}^{L} f(x)\cos\left(\frac{n\pi x}{L}\right)dx \quad n=1,2,3,\ldots \\ b_n = \dfrac{1}{L}\displaystyle\int_{-L}^{L} f(x)\sin\left(\frac{n\pi x}{L}\right)dx \quad n=1,2,3,\ldots \end{cases} \quad (4)$$

The first step is to obtain the coefficients a_0, a_n, and b_n. This is the most challenging part. After the coefficients are obtained, simply plug them into the top equation. The result is a series that can approximate the function. One nice thing about describing a function as a series is that a computer can be easily programmed to evaluate it.

Since the discontinuities have a waveform, the methods used to express waves can simulate discontinuities. **Figure 3** shows several discontinuities in which a wave-like state can be observed, so discontinuities can be demonstrated using the Fourier series equations.

According to the application of the Fourier series, we can show all joints in a mathematical form by using the Fourier series. In this research, the best Fourier series equations are calculated with determined terms and re-

Table 2: The RMSE of fitting of ten joints for several terms

	1	2	3	4	5	6	7
J1	0.0436	0.0417	0.0389	0.0196	0.0165	0.0149	0.0149
J2	0.0144	0.0134	0.0123	0.0125	0.113	0.0096	0.0082
J3	0.0274	0.0254	0.0186	0.0171	0.0145	0.0133	0.0133
J4	0.0107	0.0097	0.0090	0.0088	0.0077	0.0058	0.0050
J5	0.1112	0.0897	0.0643	0.0587	0.0580	0.0579	0.0578
J6	0.0209	0.0213	0.0110	0.0110	0.0103	0.108	0.0111
J7	0.0938	0.0745	0.0749	0.0740	0.0765	0.0796	0.0803
J8	0.0506	0.0335	0.0330	0.0330	0.0347	0.0339	0.0323
J9	0.0418	0.0426	0.0220	0.0220	0.0206	0.0216	0.0223
J10	01219	0.0969	0.0974	0.0962	0.0995	0.1034	0.1044

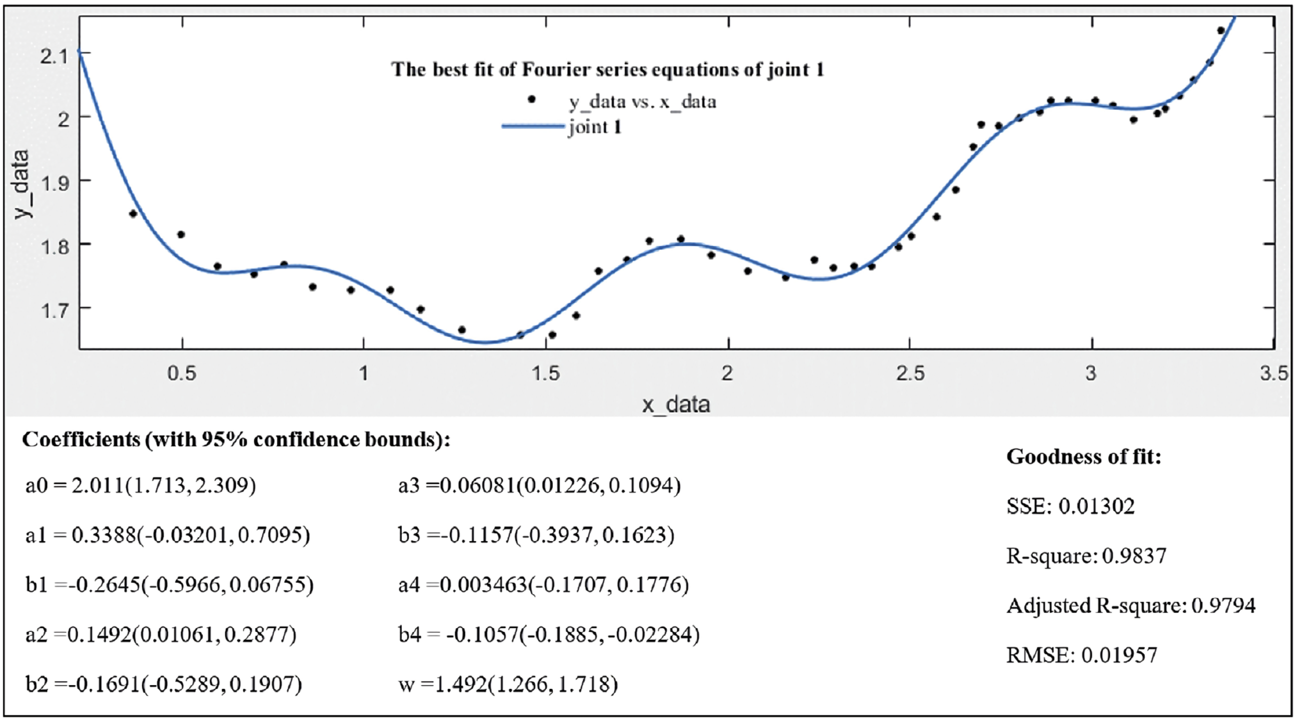

Figure 7: Schematic representation of the best fit of Fourier series equations of Joint 1

lated coefficients by fitting the Fourier series with determining terms to obtain data from digitizing joints. The fitting tests measure the compatibility of obtained data with a theoretical Fourier series with determined terms. The approximation accuracy of finding the best Fourier series equations increase by increasing the number of Fourier series terms. Finding the best Fourier series equations is subject to the best selection of Fourier series terms and the associated coefficients. An alteration procedure should be used to achieve this purpose so that the equation root mean square error (RMSE) reaches the acceptable threshold. By decreasing the RMSE, the Fourier series equation is closer to the equation of the rock joints.

The best Fourier series equation was calculated with determined terms and related coefficients for all digitized joints in the mine bench. The RMSE of fitting the Fourier series equations of ten joints is shown in **Table 2**. Also, **Figure 7** to **Figure 9** show a schematic representation of the best fitting of the Fourier series equations of three joints.

In this case, the Fourier series equation with three items can be represented as follows (**Equation 5**):

$$f(x) = a_0 + a_1 Cos(xw) + b_1 Sin(xw) + a_2 Cos(2xw) + b_2 Sin(2xw) + a_3 Cos(3xw) + b_3 Sin(3xw) \quad (5)$$

In **Table 3**, the obtained coefficients of Fourier series equations of joints with the corresponding root mean square error have been shown.

According to the obtained Fourier series equations of rock joints in the bench of a marble mine, rock joint

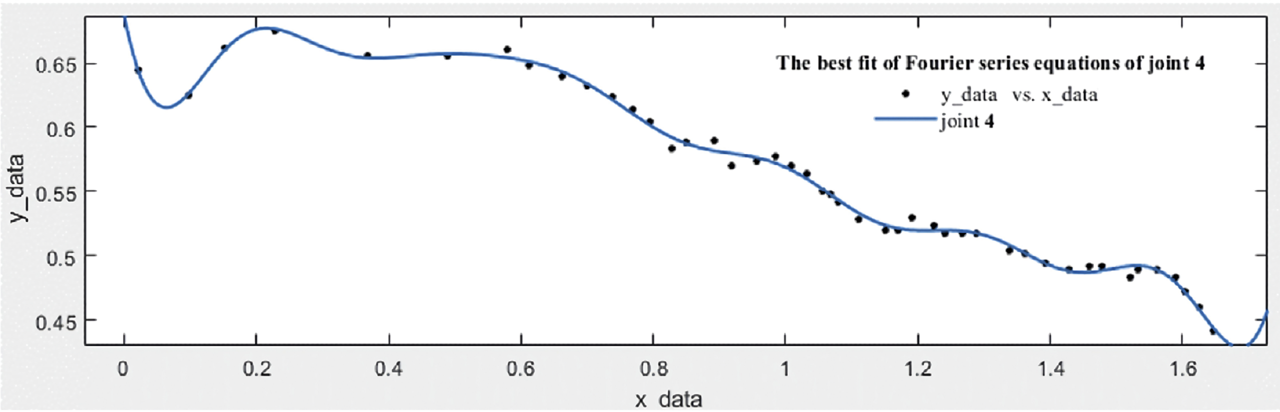

Coefficients (with 95% confidence bounds):

a0 =0.7537(0.05173, 1.456)
a1 =0.3096(-0.63, 1.249)
b1 =-0.1409(-1.164, 0.8826)
a2 =0.06085(-0.07703, 0.1987)
b2 =-0.3003(-1.503, 0.902)
a3 =-0.1271(-0.9284, 0.6742)
b3 =-0.2215(-0.7765, 0.3335)
a4 =-0.1786(-0.8488, 0.4916)
b4 =-0.05622(-0.2412, 0.1288)
w = 2.774(2.297, 3.251)

Goodness of fit:

SSE: 0.0007146
R-square: 0.9961
Adjusted R-square: 0.9941
RMSE: 0.004964

Figure 8: Schematic representation of the best fit of Fourier series equations of Joint 4

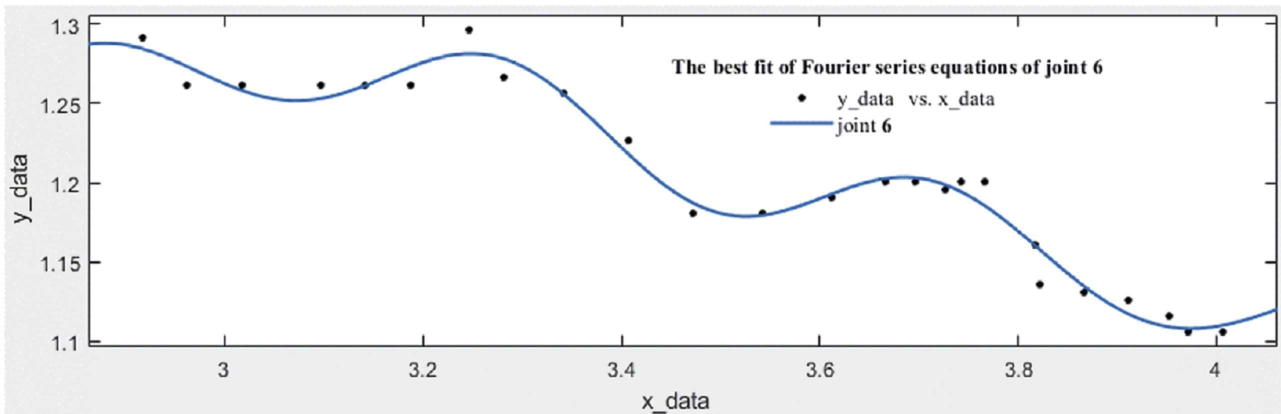

Coefficients (with 95% confidence bounds):

a0 =1.207(0.9451, 1.469)
a1 =0.06233(-0.5943, 0.7189)
b1 =-0.03934(-1.295, 1.217)
a2 =-0.021(-0.07851, 0.03651)
b2=-0.003404(-0.7399, 0.733)
a3 =0.01768(-0.2164, 0.2518)
b3 =0.002077(-1.224, 1.228)
a4 =0.01531(-1.047, 1.078)
b4 =0.008525 (-1.384, 1.401)
w =3.864(-3.362, 11.09)

Goodness of fit:

SSE: 0.001811
R-square: 0.9788
Adjusted R-square: 0.9661
RMSE: 0.01099

Figure 9: Schematic representation of the best fit of Fourier series equations of Joint 6

equations can be shown with an acceptable error rate using the Fourier series. For example, in the mentioned case study, the rock joint equations within the rock mass can be simulated by the first three Fourier series items with the RMSE approximately 0.1 to 0.2.

8. Introducing the mathematical model to represent joints morphology

A force generates a joint, and depending on the force that creates the joint, the joint wants to grow, but the re-

Table 3: The coefficients of the Fourier series equations of the joints of Block 6 (only those joints shown in which both ends are visible).

	R^2	RMSE	w	a_0	a_1	b_1	a_2	b_2	a_3	b_3
1	0.984	0.0196	1.759	1.837	0.1272	-0.103	0.02045	-0.03557	-0.02725	-0.008264
2	0.992	0.0123	-0.170	0.0210	-3.87E+10	-4.14E+09	1.525E+10	3.301E+09	-2.47e+09	-8.18E+08
3	0.919	0.0186	0.0349	-2.95E+13	4.434E+13	1.103E+12	-1.77E+13	-8.82E+11	2.95E+12	2.20E+11
4	0.983	0.009	0.1271	-9.75E+11	1.463E+12	3.273E+10	-5.85E+11	-2.61E+10	9.74E+10	6.54E+09
5	0.980	0.0643	3.626	1577	409	304	-250	-158	165	33
6	0.976	0.0110	4.402	1.216	0.0318	0.0597	0.0226	0.0076	0.0497	-0.02448
7	0.954	0.0749	-0.248	3.799E+12	-5.01E+12	-2.70E+12	1.254E+12	1.904E+12	-3.35E+10	-3.78E+11
8	0.985	0.033	0.251	2.04E+12	-2.6E+12	-1.5E+12	6.31E+11	1.08E+12	-4.9E+09	-2.1E+11
9	0.976	0.022	4.402 3.50E+12	3.50E+12	-4.77E+12	-1.87E+12	1.40E+12	1.32E+12	-1.14E+11	-2.63E+11
10	0.954	0.0974	-0.224	4.96E+12	-6.88E+12	-2.19E+12	2.16E+12	1.55E+12	-2.22E+11	-3.12E+11

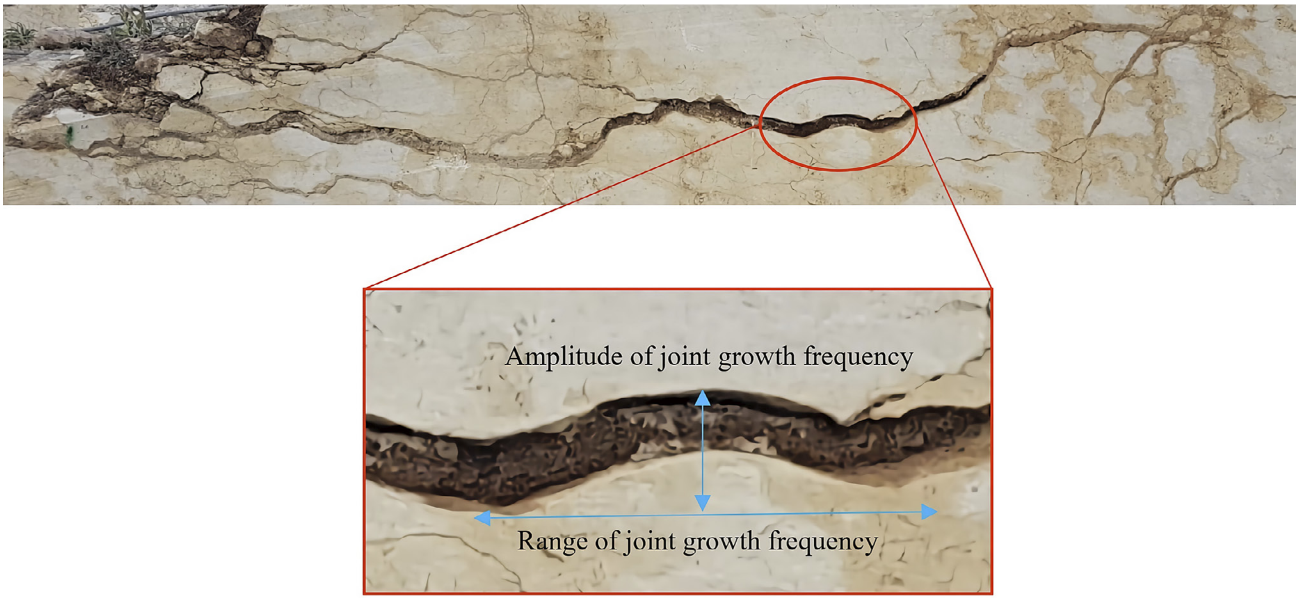

Figure 10: The morphology of the joint development and the magnification mode of the wave-like form of the joint (this joint is selected from Block 6 in Bench one from the Sarchawa marble mine).

sistance of the material will prevent the joint growth. Due to the morphology of the joints in various types of rocks, it can be seen that the joints have a wave-like state. Therefore, if we consider the joint as a wave, and according to what has been said, the material's resistance force will prevent the joint's growth, in each period of the development of the joint, both the amplitude and the range decrease. So, the resistive force of the material reduces the oscillation of the joint growth equation, and finally, damping will occur. In Figure 2, the general form of damping is shown. According to the conducted analysis of the collected data from the Sarchawa marble mine, it is concluded that the growth of the joints follows a specific relation that depends on the type of rock and the conditions under which the joints are created. In **Figure 10**, the morphology of joint development and the magnification mode of the wave-like form of the joint is shown. Also, as explained in the previous section, due to the strength of the material in the joint growth process, damping would occur.

8.1 Examining a simple mode of joint growth

To show the joint's growth, we must consider the growth of the joint in both the positive and negative directions of the coordinate system. According to surveys, the joint's growth for each period is expressed as an equation. Also, the morphology of the complete growth of the joint is shown in **Figure 11**. It is worth noting that the growth of the joint in **Figure 11** is shown based on a hypothetical theory that is based on experimental observations. It also shows that the joint growth period continues until the resistive force of the material overcomes the force which creates the joint, and then the growth of the joint is stopped.

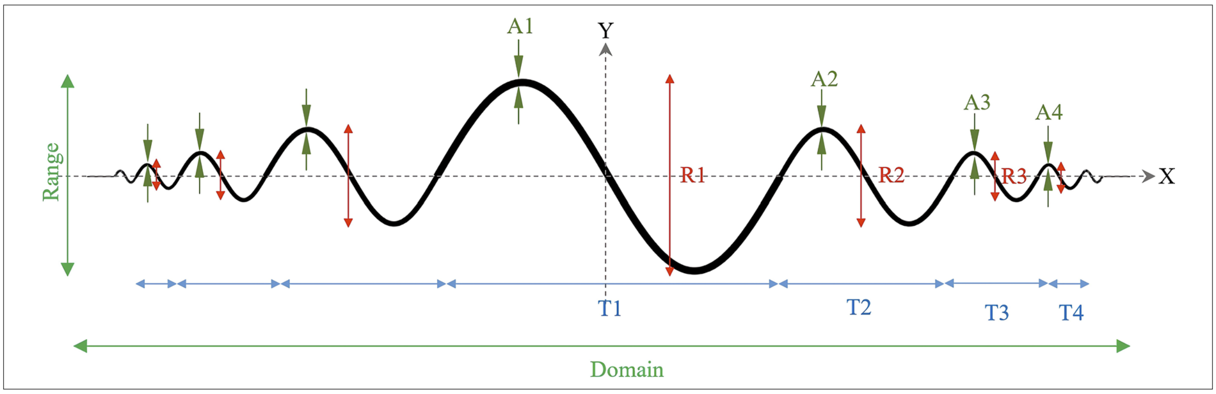

Figure 11: The complete growth of the joint and the morphological details of the joint growth morphology graph

According to the analysis of the joints of the Sarchawa marble mine, it is concluded that an equation of Fourier can represent the equation of each period of joint growth with coefficients that depend on rock type and the depth of the joint where it formed. Now, if in the first period of the joint growth, its period is equal to T, we can show the morphology equation of the joint as **Equation 6**:

$$f(x) = c + dCos(wx) + eSin(wx) \quad 0 \ll x \ll T \tag{6}$$

Where:

c, d, e, and ω – coefficients,

T – period of joint function.

These coefficients are obtained by fitting the best Fourier function to the first period of the joint growth function. It must be mentioned that the values of these coefficients depend on rock type and the depth of the joint which is formed. Since we deal with the morphology of joint growth in this section of the study, we need to know the characteristics of the joint growth graph; for this purpose, the morphological details of its morphology graph are shown in **Figure 11**.

In **Figure 11**, T_n is the periodic period for the n[th] stage of the joint growth, R_n is the range of joint growth function for the nth stage, and A_n is the aperture of joint growth function for the nth stage. The particular set of values that a function can take as input is called its domain, and this value is equal to the apparent length of the joint that is measured and taken to carry out in rock engineering works. Also, the range of the function is the set of outputs that a function can generate, given its domain. In the joint growth graph, range is the maximum value caused by the joint growth function and is equal to the first period (T_1).

According to the performed studies, it can be concluded that the first period of joint growth follows **Equation 6**. By fitting the best Fourier equation to digitalized data of the first stage of the joint growth graph in MATLAB software, c, d, e, and ω are obtained. But the general relation for the expression of the rock joint growth equation can be shown as follows (**Equation 7**):

$$y_n = c_n + d_n Cos\left(\left(\beta^{n-1}\right)wx\right) + e_n Sin\left(\left(\beta^{n-1}\right)wx\right)$$
$$n = 1.\ 2.\ 3.\ldots\infty \tag{7}$$

Where:

n – number of fluctuations of joint growth,

ω – coefficient,

c_n, d_n, e_n, α, and β – coefficients that are calculated as **Equation 8 to Equation 12**:

$$c_n = \frac{c_1}{\alpha^{n-1}\beta^{n-1}} \tag{8}$$

$$d_n = \frac{d_1}{\alpha^{n-1}} \tag{9}$$

$$e_n = \frac{e_1}{\alpha^{n-1}} \tag{10}$$

$$\alpha = \frac{R_n}{R_{n-1}} \quad 0 < \alpha \ll 1 \tag{11}$$

$$\beta = \frac{T_{n-1}}{T_n} \quad 1 \ll \beta < \infty \tag{12}$$

Where:

Rn – the range of joint growth function for the n[th] stage,

T_n – the periodic period for the nth stage of the joint growth and calculated as **Equation 13**:

$$T_n = \frac{T}{\left(2^{n-1}\right)} \tag{13}$$

For each period of joint growth, we need to determine the domain of the stage, which the domain of each period (x_n) of joint growth is calculated by **Equation 14**:

$$\sum_{i=1}^{n} T_i \ll x_n \ll \sum_{i=1}^{n-1} T_i \tag{14}$$

Until this stage, the equation for the growth of the joint in two-dimensional has been determined. Now, the question is, what is the magnitude of the joint development and the number of fluctuations in the joint growth equation? As shown schematically in **Figure 11**, it can be seen that the joint opening (aperture) decreases at each stage of the oscillation. Using aperture variations, the number of fluctuations and the length of the joint growth will be calculated. In the following, calculating the number of changes and the length of the joint development will be explained.

As mentioned, the joint opening decreases during joint growth and reaches zero at a certain joint length. As the joint opening reduces following a regular process, the decreasing ratio in the opening can be achieved in each period of joint growth. The decreasing ratio is calculated by **Equation 15**:

$$\Psi = \frac{A_{n-1}}{A_n} \tag{15}$$

Where:

Ψ – the decreasing ratio of joint aperture,

An – the aperture of joint growth function for the nth stage.

As stated, the purpose of calculating the decreasing ratio of the opening is to calculate the number of fluctuations of joint growth and finally calculate the length of the joint. We must obtain "n" in **Equation 7**. To calculate n, the initial opening value (A_1) must be measured, and the final value of the opening entered into the calculation is considered for (A_n). According to **Equation 15**, so **Equation 16** can be reached:

$$A_n = \frac{A_1}{(\Psi^{n-1})} \tag{16}$$

By rewriting **Equation 16**, so **Equation 17** is reached:

$$\Psi^{n-1} = \frac{A_1}{A_n} \tag{17}$$

Now, take the Ln of each side of **Equation 17**, so **Equation 18** is:

$$Ln\left(\Psi^{n-1}\right) = Ln\left(\frac{A_1}{A_n}\right) \tag{18}$$

By rewriting the simplified form of the left side of **Equation 18**, then **Equation 19** is attained:

$$\left(n-1\right)Ln\left(\Psi\right) = Ln\left(\frac{A_1}{A_n}\right) \tag{19}$$

Divide both sides of **Equation 19** into $Ln(\Psi)$, so **Equation 20** is obtained:

$$\left(n-1\right) = \frac{Ln\left(\frac{A_1}{A_n}\right)}{Ln\left(\Psi\right)} \tag{20}$$

By simplifying each side of **Equation 20**, so **Equation 21** is found:

$$n = \frac{Ln\left(\frac{A_1}{A_n}\right)}{Ln\left(\Psi\right)} + 1 \tag{21}$$

Finally, by simplification of the above equation, the calculation equation of "n" is obtained by **Equation 22**:

$$n = \frac{Ln\left(A_1\right)}{Ln\left(\Psi\right)} - \frac{Ln\left(A_n\right)}{Ln\left(\Psi\right)} + 1 \tag{22}$$

Given the zero value for the final value of the opening (A_n), and we know that a value of Ψ is always more than 1. We rewrite **Equation 22**. Therefore, **Equation 23** is obtained:

$$n = \frac{Ln\left(A_1\right)}{Ln\left(\Psi\right)} - \frac{Ln\left(0\right)}{Ln\left(\Psi\right)} + 1 \tag{23}$$

We know that $Ln\left(0\right) = -\infty$, and $Ln\left(\Psi\right) = \infty$, so we rewrite **Equation 23** as **Equation 24**:

$$n = \frac{Ln\left(A_1\right)}{Ln\left(\Psi\right)} - \left(-\infty\right) + 1 \tag{24}$$

and $\frac{Ln\left(A_1\right)}{Ln\left(\Psi\right)} = \infty$, finally, the value of n is: $n = +\infty$

So, if we consider the final opening zero, the infinite amount (-∞) is obtained for n, which is not scientifically acceptable. This indicates that the material which contains the joint has no resistance, which is impossible in the real world. It is clear that any force generating the joint due to the strength of the material is damping and ultimately reaches zero. So, to achieve the research goal, we consider a value close to zero for the last value of the joint aperture.

If we consider the value of the final aperture equal to one nanometer (A_n=1nm), we will have:

$$Ln\left(0.000000001\right) = -20.7233 \cong -21$$

So, we can rewrite **Equation 23** as **Equation 25**:

$$n = \frac{Ln\left(A_1\right)}{Ln\left(\Psi\right)} - \frac{21}{Ln\left(\Psi\right)} + 1 \tag{25}$$

For example, if $A_1 = 5\ mm$, $A_n = 1\ nm$ and $\Psi = 2$. Therefore, the value of n is 24.

This length is the image of the natural joint length, not the actual length of the joint. The actual length of the joint is the length of the joint curvature from O to D, which the mathematical relationship can calculate. The arc length along a curve, y= f(x), from a to b, is given by **Equation 26**:

$$Arc\ Length = \int_a^b \sqrt{1 + \left(\frac{dx}{dy}\right)^2}\, dx \tag{26}$$

The expression inside this integral is simply the length of a representative hypotenuse.

9. Discussion

Finding the model of rock joints has been proposed for about 40 to 50 years. To describe 3D simulations of rock masses, various researchers developed their techniques to introduce the joint models and finally simulate jointed rock masses. The exact morphology of joints

Table 4: Quantitate example of morphological parameters of joints profile in the Sarchawa marble mine

Morphological parameters of joints profile	Quantitate examples of the morphological model of joints				
	Example 1	Example 2	Example 3	Example 4	Example 5
D	0.93	1.70	1.94	1.98	2.74
T_1	0.36	0.24	0.4347	0.5802	0.3864
T2	0.12	0.0937	0.0905	0.2074	0.1634
R_1	0.1183	0.0889	0.1031	0.1217	0.1070
R2	0.0516	0.0375	0.0225	0.0514	0.0386
A_1	0.0452	0.0177	0.0094	0.0181	0.0164
A2	0.0177	0.0104	0.0042	0.0072	0.0055
α	0.4362	0.4218	0.2182	0.4223	0.3607
β	3.0000	2.5614	4.8033	2.7975	2.3647
Ψ	2.5537	1.7019	2.2381	2.5139	2.9818
ω	7.5620	2.0280	10.4900	37.4600	25.5800
c_1	-1.0640	4.7650	-0.0222	-2.5890	-2.7960
d_1	-0.0425	-2.6700	-1.8360	-0.0017	0.00511
e_1	-0.0964	-5.9140	-0.0807	-0.0182	-0.0315
Where: D is the depth at which the joint is formed					

present in rock masses is very complex. Therefore, due to its complexity, there is no unified terminology for joint morphology. The most convenient joint model is obtained by referencing with a model such as a circle, ellipse, polygon, or rectangle. However, these models have significant limitations, as follows:

About the applicability showed that each model corresponds to actually encountered rock mass geometries. The selection of an appropriate model in a particular case is of interest to the user and possibly not satisfactory at present. This has to be done subjectively; it is not the direct result of field sampling procedures. Following the selection, it is possible and necessary to compare the statistics of the model simulation with the sampled statistics and then update the model selection.

Representing the joint geometry of rock masses can, at present, not be done by explicitly describing each joint within a particular rock mass volume. Therefore, rock joints are usually represented as an assemblage with stochastic character, possibly even further simplified to regular assemblages (**Dershowitz and Einstein, 1988**).

All introduced models simulate the joint profile linearly; this is far from the real inherent of a rock joint. The drawbacks inherent in the traditional models significantly impact the quantity and quality of joint data and will inevitably affect our understanding of the joint influence on rock mass behaviour.

Therefore, the use of joint morphology concurrently may solve this issue; however, this task is very challenging because the mathematical modeling of rock joint morphological profile is very complicated. Consequently, mathematical methods would be helpful for rock mass simulation to determine the morphological profile of joints and their characteristics.

According to the calculations done for the joint growth in the Sarchawa marble mine, In the following, some real examples of the introduced model have been shown (see **Table 4**).

From an engineering perspective, an appropriate number of case studies must be analyzed to obtain relevant and confident results. It is hoped that in future studies, by using the mathematical morphological profile of joints, it will be possible to simulate the three-dimensional state of joints. Finally, it will be possible to simulate the jointed rock masses. In this regard, a series of studies have been conducted, and their results will be presented in the following articles.

10. Conclusion

Describing rock joint network systems has become substantial attention for researchers and engineers in different fields related to rock masses such as oil and gas, geothermal, and nuclear waste disposal during the last two decades because geometric characteristics of rock joints control the stability of structures that are built inside or on top of rock masses.

The success of a rock engineering project mainly depends on how well the joints are characterized and considered in the design and construction. The most important thing to be considered is the actual morphology of the joint because the morphology of the joint affects all calculations of rock engineering designs. The meaning of joint morphology is its true form. Unfortunately, due to the difficulty of the subject, it has not yet investigated the actual morphology of the joint. Many researchers have presented several simple forms of joint models, which introduced models far from the exact joint morphology.

The propagation of stress inside the rock follows the wave propagation rules. Also, the morphology of joints in all types of rocks follows the wave-like state. Also, using the Fourier series, a function can be described as a sum of sine and cosine waves with different frequencies and amplitudes. Since joints have waveforms, Fourier series equations can be used to represent the joints.

According to the application of the Fourier series, we can show all joints in a mathematical form by using the Fourier series. In this research, the best Fourier series equations are calculated with determined terms and related coefficients by fitting the Fourier series with determining terms to obtain data from digitizing joints. According to the Fourier series equations of rock joints in the bench of a marble mine, rock joint equations can be shown with an acceptable error rate using the Fourier series. For example, in the mentioned case study, the rock joint equations within the rock mass can be simulated by the first three Fourier series items with the root mean square error of approximately 0.1 to 0.2. Consequently, using the Fourier series equations, the mathematical equations of the joint morphological profile of the Sarchawa marble mine have been derived. To verify the validity of the research, a series of joints has been shown mathematically using the obtained equation. Finally, the results of this work clearly show that each rock joint's morphology can be expressed as a mathematical equation.

Acknowledgements

The authors would like to thank all persons for their help in collecting joint geometry properties.

Funding

The authors received no financial support for this article's research, authorship, and publication.

11. References

Agterberg, E.P. (1976): Geomathematics. New York: Elsevier, 596 p.

Ambarcumjan, R. (1974): Convex Polygons and Random Tessellations. Stochastic Geometry, 176-191.

Baecher, G.B. (1983): Statistical analysis of rock mass fracturing. Mathematical Geology 15, 329–348. https://doi.org/10.1007/BF01036074.

Baecher, G., Lanney, N. (1978): Trace Length Biases in Joint Surveys. Paper presented at the 19th U.S. Symposium on Rock Mechanics (USRMS), Reno, Nevada.

Barton, C.C. (1983): Systematic Jointing in the Cardium Sandstone Along the Bow River, Alberta, Canada; https://corescholar.libraries.wright.edu/ees/73.

Black, J.H. (1994): Hydrogeology of fractured rocks, a question of uncertainty about geometry. Applied Hydrogeology, (3)94, 56–70, https://doi.org/10.1007/s100400050049.

Becker, I., Koehrer, B., Waldvogel, M., Jelinek, W., Hilgers, C., (2018): Comparing fracture statistics from outcrop and reservoir data using conventional manual and t-LiDAR derived scanlines in Ca2 carbonates from the Southern Permian Basin, Germany, Marine and Petroleum Geology, 95, 228–245. https://doi.org/10.1016/j.marpetgeo.2018.04.021.

Berkowitz, B., (1995): Analysis of fracture network connectivity using percolation theory, Mathematical Geology, 27, 4, 467–483, https://doi.org/10.1007/BF02084422.

Cacciari, P.P., Futai, M.M., (2017): Modelling a Shallow Rock Tunnel Using Terrestrial Laser Scanning and Discrete Fracture Networks, Rock Mechanics and Rock Engineering, 50, 1217–1242. https://doi.org/10.1007/s00603- 017-1166-6.

Call, R.D., Savely, J.P., and Nicholas, D.E. (1976): Estimation of Joint Set Characteristics from Surface Mapping Data. Paper presented the 17th U.S. Symposium on Rock Mechanics (USRMS), Snow Bird, Utah.

Cleary, M. (1984): Internal Progress Report on Joint Industry Research, s.l.: MIT.

Dershwitz, W. (1984): Rock Joint Systems., Thesis (Ph. D.), Massachusetts Institute of Technology, Dept. of Civil Engineering, http://hdl.handle.net/1721.1/27939.

Dershwitz, W., Einstein, H.H. (1988): Characterizing rock joint geometry with joint system models, Rock Mechanics and Rock Engineering, 21,21–51, https://doi.org/10.1007/BF01019674.

Einstein, H. H., Baecher, G. B., Veneziano, D., Chan, H.C., Dershowitz, W.S. (1980): Risk Analysis for Rock Slopes in Open Pit Mines, Massachusetts Inst. of Tech., Cambridge. Dept. of Civil Engineering.; Bureau of Mines, Washington, DC.

Feng, Q. (2012): Practical Application Of 3d Laser Scanning Techniques to Underground Projects, A part of ISRM-Swedish national task: "A survey of 3D laser scanning techniques for application to rock mechanics BeFo Report 114, Stockholm, ISSN 1104 – 1773.

Flynn, Z., Pine, R. (2007): Fracture characterization is determined by the numerical modeling analyses. London, Taylor & Francis Group.

Grasselli, G., Egger, P. (2003): Constitutive law for the shear strength of rock joints based on three-dimensional surface parameters. International Journal of Rock Mechanics and Mining Sciences, 40, 1, 25-40, https://doi.org/10.1016/S1365-1609(02)00101-6.

Griffith, A. (1921): The Phenomena of Rupture and Flow in Solids. Philosophical Transactions of the Royal Society of London, Volume 221, pp. 163-198, https://doi.org/10.1098/rsta.1921.0006.

Harrison, J., Hudson, J. (2000): Engineering Rock Mechanics. s.l.: Elsevier Science: Oxford, ISBN, 978-0-08-043864-1, https://doi.org/10.1016/B978-0-08-043864-1.X5000-9.

Hudson, J., Harrison, J. (1997): Engineering rock mechanics: an introduction to the principles. 1th ed. s.l.:Perhamon, https://doi.org/10.1016/B978-0-08-043864-1.X5000-9.

Jing, L., (2003): Review of Techniques, Advances and Outstanding Issues in Numerical Modelling for Rock Mechanics and Rock Engineering. International Journal of Rock

Mechanics & Mining Sciences, 40, 283-353, https://doi.org/10.1016/S1365-1609(03)00013-3.

Meyer, T, Einstein, H. H., and Ivanova, V., (1999): Geologic stochastic modeling of fracture systems related to crustal faults, in Vouille, G., and Berest, P., eds., Proceedings of the 9th International Congress of Rock Mechanics, Ecole des Mines, Paris, France, 1, 493–497.

Kreyszig, E. (1999): Advanced Engineering Mathematics. 10th ed., New York: Wiley.

Kulander, B., Barton, C., Dean, S. (1979): The Application of Fractography to Core and Outcrop Fracture Investigations, s.l.: Morgantown Energy Research Center, 174 pages.

Lama, R., Vutukuri, V. (1978): Handbook on Mechanical Properties of Rocks- Testing Techniques and Results. s.l.:s.n.

La Pointe, P. (1980): Analysis of the Spatial Variation in Rock Mass Properties Through Geostatistics Paper presented at the 21st U.S. Symposium on Rock Mechanics (USRMS), Rolla, Missouri.

Lavenu A.P.C., Lamarche, J., (2018): What controls diffuse fractures in platform carbonates? Insights from Provence (France) and Apulia (Italy), Journal of Structural Geology, 108, 94–107. doi: 10.1016/j.jsg.2017.05.011.

Li, L., Huang, B., Li, Y., Hu, R., Li, X., (2018): multi-scale modelling of shale laminas and fracture networks in the Yanchang formation, Southern Ordos Basin, China, Engineering Geology. 243, 231–240. https://doi.org/10.1016/j.enggeo.2018.07.010.

Li, X., Zhang, P., He, Z., Huang, Z., Cheng, M., Guo, L., (2017): Identification of geological structure which induced heavy water and mud inrush in tunnel excavation: A case study on Lingjiao tunnel, Tunnelling and Underground Space Technology, 69, 203–208. https://doi.org/10.1016/j.tust.2017.06.014.

Liu, W.-k., Wang, R.-f., Zheng, X.-j. (2008): Estimating coal reserves using a support vector machine. Journal Of China University of Mining & Technology, 18, 103-106, https://doi.org/10.1016/S1006-1266(08)60022-X.

Matheron, G. (1975): Random Sets and Integral Geometry. New York, John Wiley & Sons, Pages: 261.

Miller, S. (1979): Determination of Spatial Variation in Fracture Set Characteristics by Geostatistical Methods, Tucson: University of Arizona, http://hdl.handle.net/10150/558020.

Park, J.W., Song, J.J., (2009): Numerical simulation of a direct shear test on a rock joint using a bonded-particle model. International Journal of Rock Mechanics and Mining Sciences, 46, 8, 1315-1325, DOI: 10.1016/j.ijrmms.2009.03.007.

Priest, S. (1993): Discontinuity Analysis for Rock Engineering. London: Chapman & Hall, DOI: https://doi.org/10.1007/978-94-011-1498-1.

Renshaw, C. E., (1998): Sample bias and the scaling of hydraulic conductivity in fractured rock, Geophysical Research Letters, 25, 1, 121–124, https://doi.org/10.1029/97GL03400.

Roberds, W. J. (1979): Numerical modeling of jointed rock. Massachusetts Institute of Technology, Department of Civil Engineering.

Santalo, L. (1976): Stochastic Geometry and Integral Calculus, Addison-Wesley.

Shakiba M., Cavalcante Filho J.S., Sepehrnoori K (2018) Using Embedded Discrete Fracture Model (EDFM) in numerical simulation of complex hydraulic fracture networks calibrated by microseismic monitoring data, Journal of Natural Gas Science and Engineering, 55:495-507. DOI: 10.1016/J.JNGSE.2018.04.019.

Swan, S. (1981): Tribology and Characterization of Rock Joints. Paper presented at the 22nd U.S. Symposium on Rock Mechanics (USRMS), Cambridge, Massachusetts.

Terzaghi, K. (1946): Rock Defects and Loads on Tunnel Supports. In: Proctor, R.V., and White, T.L., Eds., Rock Tunneling with Steel Supports, Commercial Shearing and Stamping Company, Youngstown.

Veneziano, D. (1978): Probabilistic Model of Joints in Rock, Massachusetts.: Unpublished manuscript, Massachusetts Institute of Technology, Cambridge, Massachusetts.

Wuestefeld, P., De Medeiros, M., Koehrer, B., Sibbing, D., Kobbelt, L., Hilgers, C., (2016): Automated workflow to derive LIDAR fracture statistics for the DFN modelling of a tight gas sandstone reservoir analog, 78th EAGE Conf. Exhib. 2016 Effic. Use Technol. – Unlocking Potential. https://doi.org/10.3997/2214- 4609.20160135.

Zadhesh, J., and Majdi, A. (2022b): Estimation of rock joint trace length using support vector machine (SVM). Rudarsko-Geolosko-Naftni Zbornik, 37(3), 55–64, DOI: https://doi.org/10.17794/rgn.2022.3.5

Zadhesh, J., and Majdi, A. (2022c): Estimation of Rock Joint Trace Length in Scanline Sampling Using Artificial Neural Network (ANN). NeuroQuantology, 20(8), 1616–1625, DOI: 10.14704/nq.2022.20.8. NQ44175.

SAŽETAK

Matematičko određivanje morfološkoga profila stijenskih diskontinuiteta

Određivanje geometrijskih ili morfoloških i mehaničkih svojstava diskontinuiteta te geomehanike intaktne stijene vitalno je važno pitanje u predviđanju ponašanja pri zahvatima unutar stijenskih masa ili na stijenskim masama. Morfologija diskontinuiteta važna je jer utječe na čvrstoću stijenske mase i kontrolira stabilnost struktura povezanih sa stijenskom masom. Donedavno je morfologija diskontinuiteta pojednostavnjeno sudjelovala u modelu koji je odstupao od stvarnih svojstava stijenskoga diskontinuiteta. Ovaj rad predstavlja istraživanje koje uvodi novi model za opisivanje morfologije diskontinuiteta stijena koji je vrlo blizak njegovim stvarnim svojstvima. U istraživanju je proučavan sustav diskontinuiteta u kamenolomu mramora Sarchawa. Prema istraživanju morfologija svakoga stijenskog diskontinuiteta može se izraziti matematičkom jednadžbom. Koristeći se rezultatima ovoga istraživanja, može se dobiti realističniji pogled na stijenske mase, a kao posljedica toga mogu se bolje projektirati zahvati vezani uz stijenske mase, čineći rezultat boljim i pouzdanijim.

Ključne riječi:
stijenske mase, morfologija diskontinuiteta, matematička jednadžba, kamenolom mramora Sarchawa

Author's contribution

Jamal Zadhesh (1) (Student, Ph.D., Mining Engineering) defined the idea, prepared data, analysed the data and obtained the equations governing the morphology of the rock joints, provided the interpretations, and wrote the manuscript. **Abbas Majdi (2)** (Professor, Ph.D., Mining Engineering) is the supervisor of the project and has reviewed the text of the article. He also played a significant role in problem solving and provided the interpretations and presentations of the results.